

## Mixed colloid–surfactant systems

This article has been downloaded from IOPscience. Please scroll down to see the full text article.

2004 J. Phys.: Condens. Matter 16 S1873

(<http://iopscience.iop.org/0953-8984/16/19/001>)

View [the table of contents for this issue](#), or go to the [journal homepage](#) for more

Download details:

IP Address: 129.252.86.83

The article was downloaded on 27/05/2010 at 14:36

Please note that [terms and conditions apply](#).

## Mixed colloid–surfactant systems

**O Mondain-Monval and P Poulin**

Centre de Recherche Paul Pascal—CNRS, Avenue A Schweitzer, 33600 Pessac, France

Received 23 October 2003

Published 30 April 2004

Online at [stacks.iop.org/JPhysCM/16/S1873](http://stacks.iop.org/JPhysCM/16/S1873)

DOI: 10.1088/0953-8984/16/19/001

### Abstract

We study the behaviour of colloidal particles when introduced into a liquid crystal matrix. First, we probe the influence of the surface anchoring energy by using various mixtures of surfactant and then, we investigate the influence of the nematogen shape. When the surface energy dominates, a hedgehog defect is formed and, according to an electrostatic analogy, the distortions around the particles exhibit a dipolar character. By contrast, for weaker anchoring, the configuration becomes quadrupolar as evidenced by the observation of Saturn ring defects in thermotropic systems and the structure of latex clusters in lyotropic systems. Also, the shape of the nematogens is shown to control the type of defect and interaction that take place in the system, going from a dipolar symmetry in the discotic phase to a quadrupolar one in the calamitic phase. A simple scaling analysis accounts for our findings.

### 1. Introduction

Liquid crystalline phases used as solvent for colloidal particles provide new methods of control over the spatial organization of colloidal systems. Well defined anisotropic structures and new phases have been recently observed in several systems such as mixtures of rodlike viruses and colloids [1], molecular nematic or cholesteric emulsions [2] and suspensions of latex particles in discotic micellar nematics [3, 4]. Topological defects and distortions around the particles generate inter-particle elastic forces that govern the stability and the ordering of the particles. Their surface properties impose the boundary conditions of the liquid crystal and the resultant far field distortions. The anchoring is characterized by two main features, its strength and its geometry. Limits of so called strong anchoring, with planar and normal boundary conditions, were experimentally achieved in thermotropic nematic solvents [2]. In such cases, the surface energy of the liquid crystal, about  $wR^2$ , largely dominates over the bulk elastic energy, about  $KR$ , where  $w$  is a typical anchoring energy per unit surface,  $K$  a typical nematic elastic constant [5] and  $R$  the particle radius. As a main consequence, the boundary conditions of the liquid crystal are fixed regardless of the elastic energy of the

resultant distortions. However, new behaviours are expected if the surface energy becomes weaker. The liquid crystal may adopt different orientations at the interface of the particles in order to partially relax the bulk elastic energy. In these conditions, different defects and global distortions should take place, resulting in different forms of spatial organization of colloids in liquid crystals. Also, the anchoring in thermotropic liquid crystals can be empirically controlled with the presence of adsorbed additives at the surface of the particles. In lyotropic systems, the anchoring is expected to be driven by an entropic effect which should depend on the shape of the nematogens. Consequently, it is also of critical importance to study the behaviour of colloids embedded in lyotropic liquid crystals of disclike or rodlike micelles.

The present paper is organized as follows. In the next section, we present the materials and experimental methods. In section 3.1, we investigate the role of the surface energy in the behaviour of colloids in the nematic matrix. Among the main results, we show that the symmetry of the distortions around the colloidal particles changes from dipolar to quadrupolar as the strength of anchoring or the particle size is decreased. In section 3.2, we probe the behaviour of colloids when the shape of the nematogen is disclike or rodlike. We show that a quadrupolar symmetry is observed when the micelles are rodlike whereas dipolar symmetry occurs when micelles are disclike.

## 2. Experimental details

### 2.1. Materials

To investigate the role of the anchoring strength on the behaviour of the dispersions we have worked with two different types of system. The first one consists of small latex particles, with a diameter of 50 nm suspended in a lyotropic liquid crystal, which is a solution of 53% by weight of caesium perfluorooctanoate (CsPFO) in a mixture of glycerol and water (30 wt% glycerol). This system has a phase sequence going from lamellar to a micellar discotic nematic ( $T_{LN} = 28\text{ }^{\circ}\text{C}$ , with micelles having a size of around 5 nm) and isotropic phase ( $T_{NI} = 35\text{ }^{\circ}\text{C}$ ) with increasing temperature [6]. The concentration of latex particles in the liquid crystal phase is fixed at 2% by weight. A remarkable feature of this system is that the particles, which are fully dispersed in the isotropic phase, remain dispersed in the nematic phase between  $T_{NI}$  and  $32\text{ }^{\circ}\text{C}$  ( $T_{NI}-3\text{ }^{\circ}\text{C}$ ) [3]. Below  $32\text{ }^{\circ}\text{C}$ , the particles form a random texture that can be observed using optical microscopy. However, in order to fully characterize more precisely the kinds of arrangement of the latex particles in this texture, we have used freeze–fracture transmission electron microscopy (FFTEM). This latter method is described in section 2.2.

The second type of system that was used to investigate the role of the anchoring energy is made of liquid crystal-in-water (direct emulsion) and water-in-liquid crystal (inverted emulsion) emulsions. In this case, the liquid crystal is a thermotropic system made of a mixture of biphenyl molecules of which the exact composition is not precisely known (commercial name Merck E7). The main point is that it exhibits a large nematic phase temperature domain around room temperature. In the whole study, this system is used for the emulsions at room temperature, i.e. in its nematic phase, and no temperature variation is applied to this system. The direct emulsions are performed by gently shaking 5 wt% of liquid crystal (Merck E7) in an aqueous solution containing 1 wt% of a surfactant mixture including sodium dodecyl sulfate (SDS) and a copolymer of ethylene and propylene oxide (Pluronic F 68). These two surfactants are known to produce respectively strong normal or planar anchoring conditions [3]. Thus, by playing with the composition of the SDS/F68 mixture, we can continuously vary the anchoring from strong normal to strong planar anchorings. We then use these mixtures to make water-in-liquid crystal inverted emulsions by inverting the ratio

of aqueous solution (5 wt%) over liquid crystal (95 wt%). Although the used surfactants are not efficient at stabilizing water droplets in organic solvent, the low concentration of water droplets allows isolated particles to be observed before they coalesce as they collide with each other.

In section 3.2, we investigate the influence of the nematogen shape on the behaviour of the colloidal dispersion. For this purpose, we use 1.4  $\mu\text{m}$  diameter latex particles suspended in a lyotropic liquid crystal system in which both a micellar nematic phase, composed of disclike micelles (discotic nematic  $N_D$ ), and a micellar nematic phase, composed of rodlike micelles (calamitic nematic  $N_C$ ), are present in the phase diagram. The system is a ternary mixture composed of SDS, decanol (DeOH) and water. The phase diagram indeed exhibits both calamitic ( $N_C$ ) and discotic nematic domains ( $N_D$ ) [7]. We have chosen two compositions in these domains:  $N_D$  (water 66.1%; SDS 28.2%; DeOH 5.7% by weight) and  $N_C$  (water 68.9%; SDS 26.1%; DeOH 5.0% by weight). We point out that these two compositions are very close. Therefore, although being differently shaped, the micelles have almost identical interfacial properties. The 1.4  $\mu\text{m}$  latex particles are introduced in the sample at a volume fraction of approximately 1%.

## 2.2. Methods

For all the previously described systems, our first tool is polarizing optical microscopy that allows the determination of the type of liquid crystal phase exhibited by the system. To get rid of any evaporation problems, the samples are introduced in thin glass capillary tubes which are then sealed at both ends. When temperature had to be varied, i.e. for the CsPFO/water/glycerol system, these capillary tubes were put in a special oven that allows the sample to be observed while still controlling its temperature. The nature of the phases can be easily deduced from the type of observed texture that is very characteristic. The differences between the two nematic phases (for the SDS/DeOH/water system) are evidenced by looking at the samples confined between two glass slides separated by approximately 20  $\mu\text{m}$ . In the  $N_C$  phase, the micelles and the associated nematic director spontaneously align parallel to the slides (see the discussion concerning the alignment in section 3.2). Such alignment is known as planar anchoring and can be detected by rotating the sample with respect to the crossed polarizers [8]. In the  $N_D$  phase, the alignment of the micelles leads to homeotropic anchoring with the director normal to the slides. As a result, the sample is dark between crossed polarizers regardless of its relative orientation. For all the studied samples, the presence of the latex particles did not change the nature of the liquid crystal phase.

The organization of the small 50 nm latex particles in the CsPFO/water/glycerol system is observed using FFTEM. In such experiments, a small volume of the sample (around 10  $\mu\text{l}$ ) is deposited on a 5 mm<sup>2</sup> copper plate. Then, the plate is subjected to a previously chosen temperature and, once thermal equilibrium is achieved (which is very fast when working with such small volume samples), the samples are afterward quenched rapidly by plunging them into liquid propane cooled to  $-190^\circ\text{C}$  by liquid nitrogen. The presence of glycerol in the quenched samples ensures that the structure of the fluid cannot change during the cooling process. Indeed, glycerol acts as a cryoprotectant to avoid the formation of ice crystals [9]. The frozen samples are introduced into a vacuum chamber and fractured at a temperature of  $-150^\circ\text{C}$ . The replications are ensured by a shadowing of platinum, deposited at a  $35^\circ$  angle with respect to the fracture surface, followed by the deposition of a carbon film normal to the surface. The replicas are removed from the copper plate and cleaned in tetrahydrofuran to dissolve the latex particles. We observe the replica with a transmission electron microscope. The resolution of the system is limited by the size of the Pt/C grains (around 5 nm).

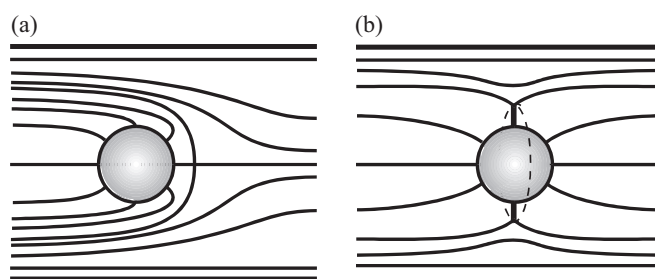


**Figure 1.** Schematic of the director field around a colloidal particle in conditions of normal (or almost normal) boundary conditions: dipolar configuration with a hedgehog defect (a); quadrupolar configuration with a disclination loop (b).

### 3. Results and discussion

#### 3.1. Role of the anchoring strength

In this section, we explore the limit of weak anchoring in systems where the ratio of  $wR^2$  over  $KR$  is lowered. We used the two different classes of composite emulsions that were described in the previous section: nematic emulsions consisting of water droplets suspended in thermotropic liquid crystal and suspensions of latex particles in CsPFO/water/glycerol lyotropic liquid crystals. In nematic emulsions, the ratio  $wR^2/KR$  is varied by changing the anchoring energy  $w$  through the use of the different surfactant molecules adsorbed at the droplet interface. The liquid crystal distortions around micrometric particles are observed using polarizing optical microscopy. In lyotropic dispersions,  $wR^2/KR$  is lowered using the smaller 50 nm particles and, looking at the FFTEM pictures, one can analyse the colloidal structures that result from elastic interactions between nanometric particles.

When the surface energy dominates, the distortions around the particles exhibit a dipolar symmetry and the particles tend to form chains aligned along the nematic director, in agreement with previous results [2, 10]. The anisotropy of the clusters is not due to the growth process in the anisotropic fluid. Instead, it is caused by the anisotropy of the interactions between the particles which are free to rearrange with respect to each other and to the nematic director in order to minimize the elastic energy.

Two possible configurations of a nematic liquid crystal around a particle are schematically drawn in figures 1(a) and (b), for a system with preferential normal boundary conditions. To satisfy the constraints that the liquid crystal is aligned far from the particle and normal to the particle surface (or almost normal for weaker anchoring), a hedgehog defect (figure 1(a)) or a disclination loop (figure 1(b)) accompanies the particle. Following an electrostatic analogy, the configuration with the hedgehog defect has a dipolar symmetry whereas the system with the disclination loop has a quadrupolar character. As experimentally [2] and theoretically [10, 11] shown, the dipolar configuration is more stable in conditions of strong anchoring. As an important consequence, particles experience dipole–dipole interaction and form long chains aligned along the nematic director, as shown with water droplets in thermotropic liquid crystals [2] or with large latex particles (larger than  $1\ \mu\text{m}$ ) in lyotropic discotic nematics [3].

First, we present the results obtained with the 50 nm latex particles suspended in the CsPFO/water/glycerol system. As discussed in section 2.1 and in [3], the latex particles remain dispersed in the nematic phase between  $32\ ^\circ\text{C}$  and  $T_{\text{NI}}$  ( $35\ ^\circ\text{C}$ ). In this temperature range, the micelle anisotropy is probably still too weak to generate elastic interactions strong

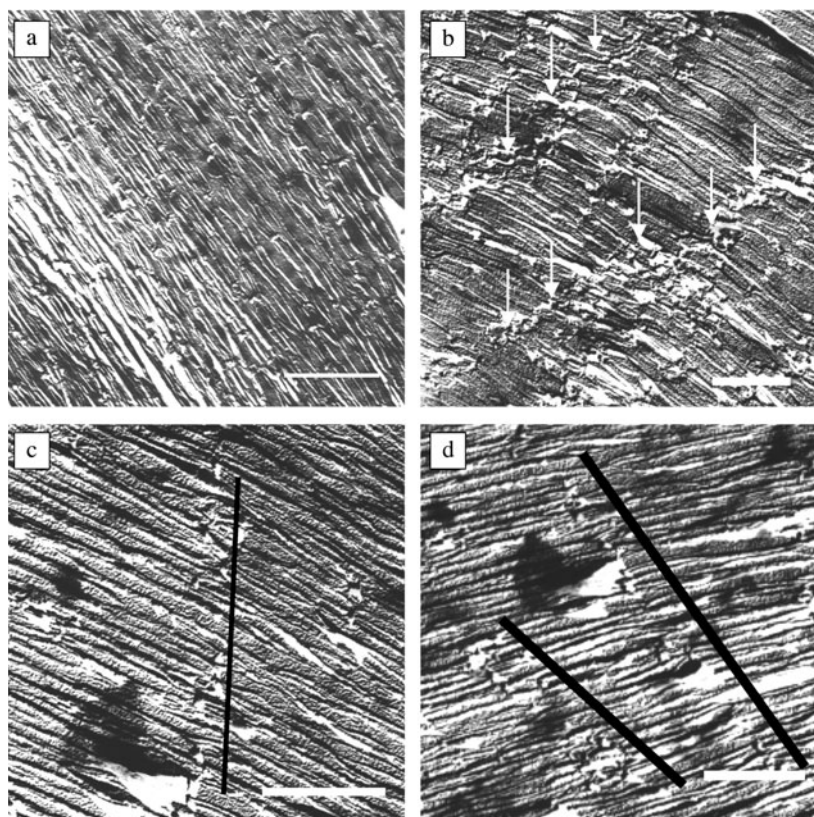


**Figure 2.** Freeze fracture transmission electron microscope picture of latex particles (50 nm) in lyotropic nematic (CsPFO 53% in water/glycerol). The particles appear as point irregularities over the stripes, reminiscent of the liquid crystal ordering. The nematic director is normal to the observed stripes (bottom right corners: white bars corresponding to 500 nm). (a) Sample frozen from  $T = 34$  °C. The particles are randomly dispersed in the nematic texture. (b) Sample frozen from  $T = 31$  °C. The particles are aggregated and form compact and elongated clusters. The white arrows points toward groups of particles belonging to the clusters. (c), (d) Samples frozen from  $T = 31$  °C. We interpret this picture as showing a few particles originating from the fracture of a large initial cluster. This allows the identification of the relative orientation of the cluster with respect to the nematic director, i.e. the normal to the stripes. Black lines parallel to the clusters are presented as guides to the eyes.

enough for a phase separation to take place. However, between 28 °C ( $T_{LN}$ ) and 32 °C, a phase transition occurs and the particles form a random texture [3] in the nematic.

Using FFTEM, the structures exhibited by this mixed system, at various temperatures, can be characterized at the nanometric scale. We now comment on the micrographs presented in figure 2. Although frozen from the nematic phase, the samples exhibit stripes which are usually observed in lamellar phases. Such stripes are also observed in samples free of particles. This indicates that the freezing step is long enough to allow local reorganization of the surfactant molecules from oblate micelles to extended bilayers. However, as shown by pictures of the high temperature sample (figure 2(a)), the latex particles are not affected by the quench, i.e. they still remain individually and randomly dispersed in the liquid crystal matrix. The surfactant bilayers resulting from the lateral fusion of the oblate micelles have their normal parallel to the initial nematic director. This allows the anisotropy of the latex clusters to be characterized

with respect to the director. Indeed, the presence of particle clusters is revealed in figure 2(b), which is a picture of the sample when quenched from an initial temperature of 31 °C. Instead of being aligned along the nematic director (i.e. perpendicular to the stripes), the long axes of the clusters seem to adopt non-zero angles with respect to the director. This effect can also be observed in some other pictures of the identically quenched system (figures 2(c), (d)). In such micrographs, the particles appear not to be aggregated but still seem to form elongated structures in which the particles are far from each other but on average oriented in a well defined direction (that we indicate with the black lines in figures 2(c) and (d)), that is once again not perfectly parallel to the optical axis. One interpretation for this picture would be that these particles originally belonged to larger clusters from which they were separated during the fracture process. Whereas they are homogeneously dispersed at 34 °C (figure 2(a)), at 31 °C the freeze–fracture technique reveals a pronounced anisotropy of the texture which is not observed using optical microscopy; the aggregates being elongated along a well defined direction. This anisotropy reflects the presence of anisotropic elastic interactions between the small particles [12]. The tilt from the normal suggests that the particles exhibit quadrupolar-like behaviour, in sharp contrast with the behaviour of larger particles in the same discotic phase [4].

To confirm these findings, we now present the results obtained with the thermotropic nematic emulsions. As previously described, water-in-liquid crystal (inverted emulsion) or liquid crystal-in-water (direct emulsion) droplets are model systems because the anchoring can be controlled using various surfactant adsorbed at the liquid crystal–water interface. The nature and the energy of the anchoring is deduced by analysing the internal configuration of liquid crystal droplets in water [13, 14]. Although the curvature of the interface is opposite from inverted to direct systems, analysis of liquid crystal droplets is helpful to find systems with weaker anchoring. Indeed, anchoring is a molecular phenomenon which is not expected to strongly depend on the curvature of micrometric droplet interfaces which can be considered as flat at the molecular scale. To clearly analyse the internal configuration of liquid crystal droplets using optical microscopy we prepare large droplets of a few tens of microns. Depending on the ratio of SDS over F68 we find different patterns. Radial or bipolar configurations are observed when the SDS ratio is above roughly 25% or below 10%. These are respectively characteristic of strong normal and planar anchoring [13]. As shown in figure 3(a), between about 10 and 25%, equatorial configurations are observed. According to previous studies [13], these patterns indicate that weak normal boundary conditions are achieved in these latter conditions.

We now discuss the case of water droplets dispersed in the liquid crystal matrix. As expected, when the SDS concentration is above 25%, dipolar patterns with hedgehog defects, characteristic of strong normal anchoring, are observed. Below 10%, bipolar droplets with boojums defects, characteristic of strong planar anchoring, are observed. Both of these configurations are similar to those reported in the literature for strong anchoring [2]. As shown in figure 3(b), a new pattern consisting of a disclination loop around the particle is observed between 10 and 25%, in conditions of weaker anchoring. Such a loop, known as a Saturn ring, provides quadrupolar symmetry to the system. We occasionally observe the coexistence of such a pattern with hedgehog defects when the SDS ratio is close to 25%, meaning that metastable states can coexist in particular anchoring conditions.

Theory [10] and computer simulations [11] show that a dipolar configuration is more stable in situations of strong anchoring. Exact calculations would be more complicated in this case because the normal boundary constraints are relaxed due to weaker anchoring. However, a simple calculation can be proposed to compare the energetic cost of quadrupolar and dipolar configurations in conditions of very weak anchoring. In this limit, a particle can be suspended in the liquid crystal without accompanying defects but still with elastic distortions. Their energetic

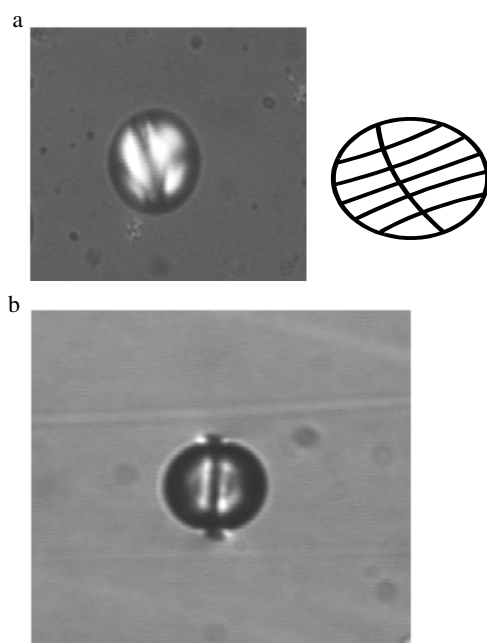


**Figure 3.** (a) Optical microscope picture between crossed polarizers of a 20  $\mu\text{m}$  liquid crystal droplet in water (surfactant solution SDS 0.2%; F68 0.8%). The liquid crystal adopts an equatorial configuration with an internal disclination loop at the surface of the particle. The director field is sketched in the schematic diagram. This pattern results from weak normal anchoring. (b) Optical microscope picture of an equatorial ring around a 0  $\mu\text{m}$  water droplet (surfactant solution SDS 0.2%; F68 0.8%) in aligned nematic. Far field horizontal orientation of the director is provided by polymer coating and rubbing of the glass slides. The normal to the equatorial ring is aligned along the horizontal axis as sketched in figure 1(b).

cost can be estimated using a single elastic constant [5]:  $E_{\text{el}} = \int_V \frac{1}{2} K [(\text{div } \mathbf{n})^2 + (\text{curl } \mathbf{n})^2] dV$ , where  $\mathbf{n}$  is the director field, aligned along the  $z$  axis at long range. Assuming multipolar fields [10] and considering the lowest order terms, we take  $n_x = p \cdot x/r^3$  and  $n_y = p \cdot y/r^3$  for the dipolar configurations and  $n_x = q \cdot x/r^5$  and  $n_y = q \cdot y/r^5$  for the quadrupolar configurations, where  $p$  and  $q$  are variational parameters and  $r$  the distance between the particle centre and a point  $M(x, y, z)$ . The surface energy is calculated using the Rapini–Papoular expression [15]:  $E_{\text{surf}} = \int_S \frac{1}{2} w (\sin \gamma)^2 dS$ , where  $\gamma$  is the angle between the director and the surface normal. Minimizing  $E_{\text{surf}} + E_{\text{el}}$  with respect to  $p$  and  $q$  gives the optimal configuration for a given size. In the limit of large  $K/wR$ , the energy of this optimum is lower for quadrupolar than for dipolar configurations. Since the dipolar configuration is more stable for infinite anchoring a transition is expected for an intermediate value of weaker anchoring. We experimentally demonstrate that the expected crossover from dipolar to quadrupolar is achieved through the formation of a Saturn ring in thermotropics. In lyotropics, the defect structure is not elucidated but the shape and the orientation of the clusters also suggest quadrupolar symmetry. These findings agree well with earlier simulations [11]. Note that the formation of a Saturn ring located at the surface of the particle is also expected. It is nevertheless difficult to conclude from our pictures whether the loop is at the surface or at a finite distance from the interface. Finally, we point out that simulations predict metastability of the Saturn ring in conditions of strong anchoring with an energy that decreases with lowering the anchoring until it becomes lower than that of the dipolar configuration. This expectation seems to be in good agreement



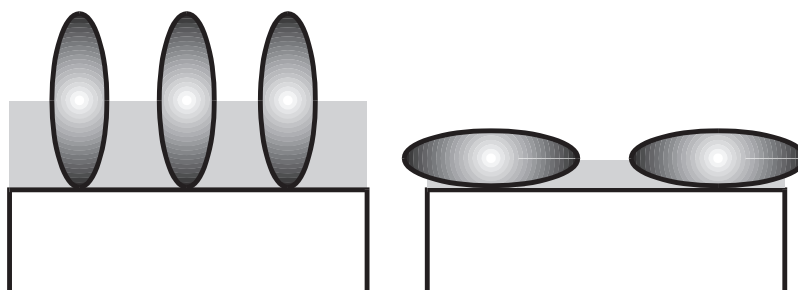


**Figure 4.** Anisotropic particles (rodlike or disclike) close to a wall. The excluded volume that is sketched by the grey area is smaller when the particles align parallel to the surface.

with the observed coexistence of Saturn rings and hedgehogs in conditions of weak anchoring. However, the absence of rings in conditions of strong anchoring indicates that the well depth and the energy barrier toward more stable dipoles are too low for Saturn rings to be observable.

To summarize, these results clearly show that distinct behaviour is observed when  $w$  is lowered in nematic emulsions or when smaller particles are suspended in lyotropic liquid crystals. In lyotropics, the particles form elongated clusters whose main axis adopts a non-zero angle with respect to the director. This observation suggests that the particles experience quadrupolar interactions instead of dipolar ones. Such a transition from dipolar to quadrupolar symmetry is clearly confirmed in nematic emulsions by the observation of a disclination loop, known as a Saturn ring, around the droplet.

### 3.2. Role of the nematogen shape in lyotropic liquid crystals

Let us just recall that, at high volume fraction, disclike or rodlike particles in solution spontaneously align in a preferential direction [5]. The resultant mesophases are known respectively as discotic or calamitic nematic phases. In discotics  $\mathbf{n}$  is parallel to the normal to the discs, whereas in calamitics it is parallel to the long axis of the rods. The stability of these phases can be understood by just considering hard core interactions between the anisotropic objects. At high volume fraction, the entropy of the system is higher in the ordered phase than in the isotropic one, the loss of rotational entropy in the nematic phase being compensated by the reduction of the excluded volume of the nematogens. In such systems, the entropy of the hard core particles should govern the alignment of the nematogens both in the bulk and at the interface of the colloidal particles [16]. As sketched in figure 4, the excluded volume of a disc or a rod at a surface is reduced when the particle is parallel to the surface. Again, this reduction is accompanied by a loss of rotational entropy. This latter contribution being weaker, rodlike and disclike nematogens are expected to align parallel to a surface. Consequently, the associated director should exhibit normal or parallel to a surface leading to distinct distortions of the nematic order around spherical particles. Due to the cost of the elastic distortions [17, 10], the particles should experience different elastic interactions and self-organize into dissimilar spatial structures.

We present the results obtained when dispersing the  $1.4 \mu\text{m}$  latex spheres in the SDS/DeOH/water lyotropic liquid crystals, both in the  $N_C$  and in the  $N_D$  phases. We can assume that in both systems the interactions are of the hard core type because the electrostatic repulsion is strongly screened due to the high ionic strength of the solutions [18]. Thus, this makes this system a good model to test the behaviour of spheres in nematic solutions of discs

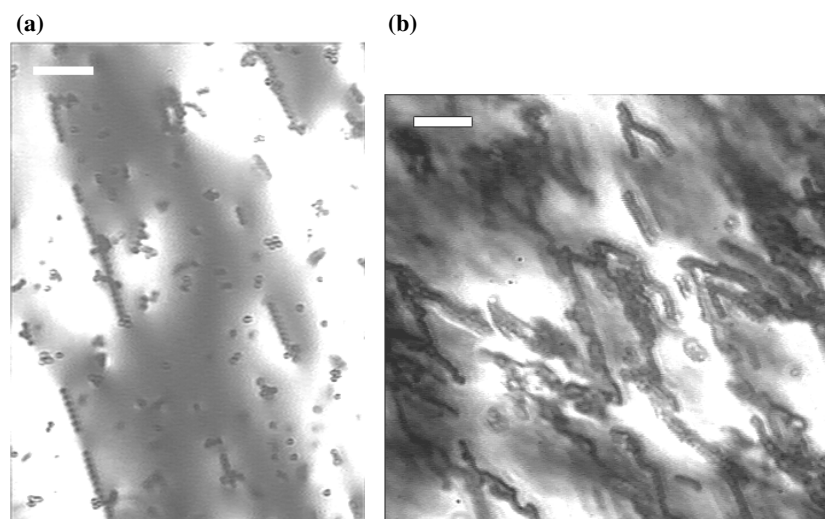


**Figure 5.** Optical microscope pictures of  $1.4\ \mu\text{m}$  latex particles in the discotic and calamitic nematic phases of the SDS/DeOH/water system. The samples are observed between crossed polarizers and contained in sealed  $100\ \mu\text{m}$  thick rectangular capillary tubes. White bar:  $15\ \mu\text{m}$ . (a) Discotic nematic phase ( $N_D$ ): the particles form long parallel chains. (b) Calamitic nematic phase ( $N_C$ ): the particles form more compact anisotropic clusters and V structures.

and rods. Instead of arising from molecular interactions as in nematic emulsions, the anchoring is here mainly due to entropic effects [4]; the excluded volume of the micelles being reduced when the discs or the rods are parallel to the interface [16]. This orientation leads to preferential normal or planar boundary conditions for the director.

The nature of the nematic phase is not affected by the presence of particles at such low volume fraction. However, due to the elastic interaction induced by the particles, a demixing is expected at equilibrium with a complete segregation between the nematic phase and the particles [3]. To avoid this segregation and suspend the latex spheres within the nematic phase, the samples are vigorously shaken. As shown in figures 5(a) and (b), the particles organize into well defined anisotropic structures within the nematic. The structures are stable over several days meaning that they are stabilized by both attractive and repulsive interactions between the colloidal spheres. In fact, such interactions arise from the orientational elasticity of the solvent and clearly depend on the nature of the nematic phase. However, observed in  $100\ \mu\text{m}$  thick capillary tubes in which the global nematic alignment cannot be controlled, the particles form chainlike structures in the  $N_D$  phase whereas they form more compact clusters in the  $N_C$  phase. By contrast with aggregates resulting from segregation [3], these clusters are anisotropic with connected chains in V-shaped arrangements. In order to fully characterize the anisotropy of the clusters with respect to the nematic director we also observed the systems in thinner samples and at the wedges of capillary tubes.

Further experiments [4] have shown that the particles form chains that align normal to the wedge of a rectangular capillary tube in the  $N_D$  phase. In this region of the sample, the nematic director is locally normal to the capillary wall. Therefore, we deduced that the long chains observed in the  $N_D$  phase are aligned along the nematic director. We have observed a similar behaviour in the  $N_D$  phase of the water/perfluorooctanoate mixture, confirming that this effect is independent of the system chemistry. The formation of chains suggests that the particles experience dipolar elastic interactions as recently reported for thermotropic liquid

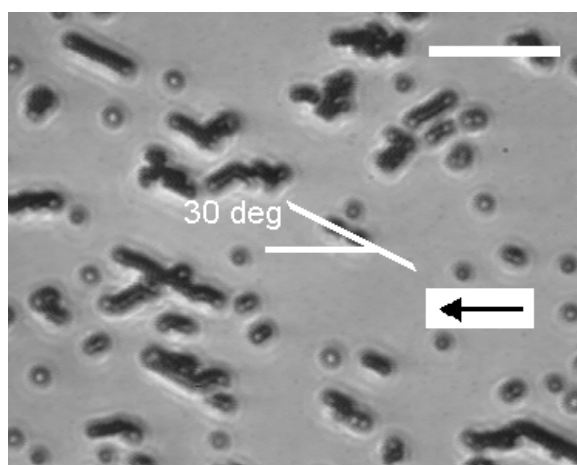


**Figure 6.** Optical microscope picture of 1.4  $\mu\text{m}$  latex particles in the  $N_C$  phase between glass slides separated by approximately 20  $\mu\text{m}$ . The director is parallel to the slides and its orientation is indicated by the black arrow. The angle between the global nematic alignment and a line joining the centre of two adjacent particles can be positive (approximately  $+30^\circ$ ) or negative (approximately  $-30^\circ$ ). In two dimensions, this results in the formation of distorted chains with the average orientation going from  $0^\circ$  to about  $\pm 30^\circ$  for the largest angles. White bar: 15  $\mu\text{m}$ .

crystals in conditions of strong normal anchoring [2]. This electrostatic analogy arises from the minimization of the elastic free energy [5]:

$$E_{\text{el}} = \int_V \frac{1}{2} [K_1 (\text{div } \mathbf{n})^2 + K_2 (\text{curl } \mathbf{n})^2 + K_3 (\mathbf{n} \times \text{curl } \mathbf{n})^2] dV,$$

where  $K_1$ ,  $K_2$ , and  $K_3$  are the nematic elastic constants. Assuming a single elastic constant [5, 10, 17], the components of the nematic director are expected to be solutions to the Laplace equation. The lowest order term and the resultant far field behaviour are set by the symmetry of the distortions around the spherical particles. As shown in figure 1, a dipolar configuration with a vector symmetry is predicted and observed in conditions of normal anchoring at the surface of the particles [17, 2, 10]. This configuration includes a topological hedgehog defect. This allows the topological constraints that the director must be normal to the particle surface and globally aligned far from the sphere to be satisfied. The first constraint indicates that any deviation from the normal anchoring conditions has an energetic cost that is dominant in this problem. Such deviation would allow less distorted configuration with lower elastic cost [11, 12]. The surface energy of a deviation can be estimated using a simple scaling argument. Having an entropic origin, it is on the order of  $k_B T/a^2$  per unit surface where  $k_B T$  is the thermal energy and  $a$  a typical micellar size (about a few nanometres [7]). The total surface energy is thus approximately  $R^2 k_B T/a^2$ , where  $R$  is the radius of the spherical particle. The other energetic contribution corresponds to the bulk elastic distortions, on the order of  $K R$ . Since  $K$  is approximately  $k_B T/a$  [5], the ratio of the elastic contribution over the surface energy is typically  $a/R$ . The spheres being much larger than the micelles, one deduces that the surface energy is much larger than the elastic one. This explains the absence of deviations from normal anchoring. Therefore, our observations confirm that the discs are parallel to the particle surface as expected from minimization of the excluded volume of the micelles [16].

The microscope picture of figure 6 shows latex particles in the  $N_C$  phase confined between two glass slides separated by approximately 20  $\mu\text{m}$ . In such thin samples, the nematic

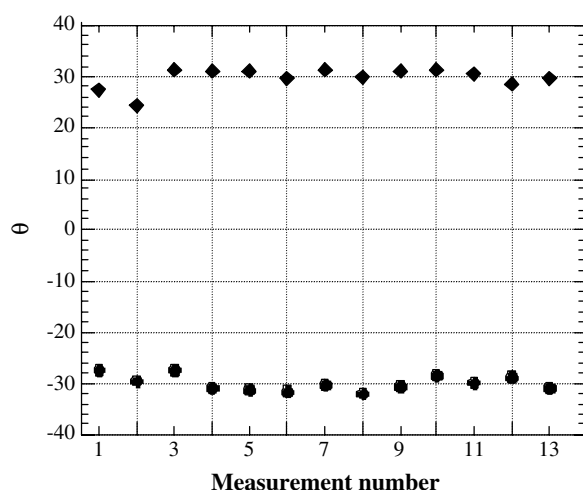


**Figure 7.** Magnitude of the largest angles between the director and long chains of particles measured on several microscope pictures similar to that of figure 6; positive and negative values are plotted as functions of the measurement number. We find approximately the same number of positive and negative values, as expected from the symmetry of the nematic phase. The average angles are equal to  $\pm 30^\circ$ .

alignment is parallel to the slides and the clusters are quasi-bidimensional. We observe chains which adopt nonzero angles with respect to the nematic alignment. We plot in figure 7 the magnitude of the largest angles measured for a series of long chains. Analysis of several pictures shows that they are roughly equal to plus or minus  $30^\circ$ . Such anisotropy reflects the quadrupolar character of the nematic distortion around the particle and of the resultant elastic interaction [2]. A quadrupolar configuration is expected in conditions of strong planar anchoring as shown in figure 8. This configuration includes two surface defects that are diametrically opposed and located at the poles of the particle (boojums defects). As in the previous case, the surface energy greatly exceeds the bulk elastic one, leading thereby to the strength of the present anchoring. To minimize the elastic distortions, the line joining the centre of two droplets makes a  $30^\circ$  angle with respect to the global nematic alignment. Consequently, in two dimensions, the formed chains exhibit this particular angle. However, this also allows the formation of more distorted structures as this angle can change sign from one droplet pair to another one. This explains the presence of elongated structures that adopt a lower effective angle with the director. Again, as deduced for the  $N_D$  phase, investigations of the  $N_C$  phase confirm that the micelles are parallel to the particle surface. In this case, the alignment leads to planar anchoring and quadrupolar interactions instead of normal anchoring and dipolar interactions.

These results clearly reveal the existence of anisotropic interparticle interactions mediated by the nematic matrix. The observed colloidal structures have different symmetry in disclike or rodlike micellar solutions. Considering a continuum description of the nematic state [5, 19], the interaction between the particles can be ascribed to the orientational elasticity of the micellar solution. Moreover, using an electrostatic analogy [17, 2], we deduce that the spherical particles experience dipolar interactions in discotic phases and quadrupolar interactions in calamitic phases. These interactions reflect different anchoring conditions and show that the associated surface energies overcome the elastic cost of the distortions.

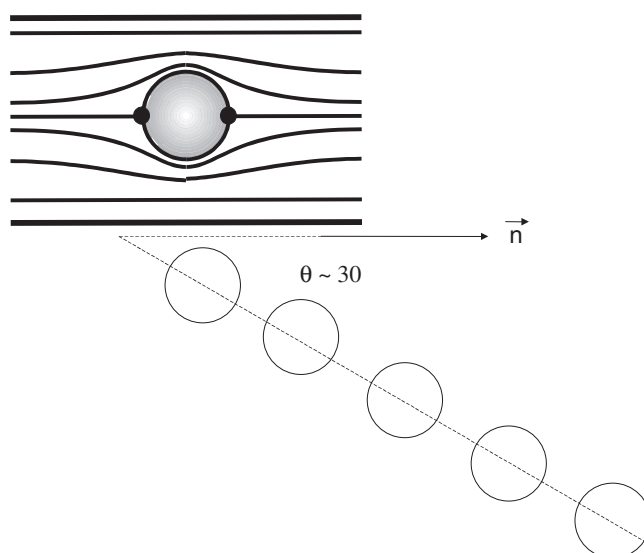


**Figure 8.** Schematic diagram of the director field around a colloidal particle in planar boundary conditions: the quadrupolar configuration has two boojums surface defects. The line joining the centre of two particles adopts an angle of  $\theta = 30^\circ$  with respect to the nematic alignment in order to minimize the elastic distortions.

#### 4. Conclusion

The surface energy plays a determinant role in the behaviour of particles suspended in liquid crystals. Varying this energy allows different colloidal structures to occur. As in classical suspensions in isotropic fluids, interactions between particles can be modulated by changing their surface chemistry or the shape of the nematogens. A unique feature of interactions in anisotropic fluids arises from the competition between bulk elastic and surface energy. This allows a control over the intrinsic nature of the interactions through the surface chemistry, the particle size and the nematogen shape, this concept providing new possibilities for the tailoring of new ordered materials.

#### Acknowledgments

Special thanks to D Weitz for his strong moral support during the course of writing this manuscript. We thank J Y Juanicot and P Richetti for technical assistance.

#### References

- [1] Adams M, Dogic Z, Keller S L and Fraden S 1998 *Nature* **393** 349
- [2] Poulin P, Stark H, Lubensky T C and Weitz D A 1997 *Science* **275** 1770  
Poulin P and Weitz D A 1998 *Phys. Rev. E* **57** 626  
Zapotocki M, Ramos L, Poulin P, Lubensky T C and Weitz D A 1999 *Science* **283** 209
- [3] Poulin P, Raghunatan V A, Richetti P and Roux D 1994 *J. Physique II* **4** 1557  
Raghunatan V A, Richetti P and Roux D 1996 *Langmuir* **12** 3789  
Raghunatan V A, Richetti P, Roux D, Nallet F and Sood A K 1996 *Mol. Cryst. Liq. Cryst.* **288** 181
- [4] Poulin P, Frances N and Mondain-Monval O 1999 *Phys. Rev. E* **54** 4384
- [5] de Gennes P G and Prost J 1994 *The Physics of Liquid Crystals* (London: Oxford University Press)

- [6] Boden N, Jackson P H, McMullen K and Holmes M C 1979 *Chem. Phys. Lett.* **65** 476
- [7] Quist P O, Halle B and Furo I 1992 *J. Chem. Phys.* **96** 3875
- [8] Figueiredo Neto A M, Galerne Y, Levelut A M and Liebert L 1985 *J. Physique Lett.* **46** L499  
Oliveira E A, Photinos P J and Figueiredo Neto A M 1993 *Liq. Cryst.* **14** 837
- [9] Gulik-Krzywicki T 1997 *Curr. Opin. Colloid Interf. Sci.* **2** 137  
Zasadzinski J A N and Bailey S M 1989 *J. Electron Microsc. Techn.* **13** 309
- [10] Lubensky T C, Pedey D, Currier N and Stark H 1998 *Phys. Rev. E* **57** 610
- [11] Ruhwandl R W and Terentjev E M 1997 *Phys. Rev. E* **56** 5561  
Stark H 1999 *Eur. Phys. J. B* **10** 311
- [12] Mondain-Monval O, Gulik-Krzywicki T and Poulin P 1999 *Eur. Phys. J. B* **12** 167
- [13] Drzaic P S 1995 *Liquid Crystal Dispersions (Series on Liquid Crystals vol 1)* (Singapore: World Scientific)  
Krajl S and Zumer S 1992 *Phys. Rev. A* **45** 2461  
Erdmann J H, Zumer S and Doane J W 1990 *Phys. Rev. Lett.* **64** 1907
- [14] Volovik G E and Lavrentovitch O D 1983 *Sov. Phys.—JETP* **58** 1159
- [15] Sonin A A 1995 *The Surface Physics of Liquid Crystals* (New York: Gordon and Breach)
- [16] Poniewierski A and Holyst R 1988 *Phys. Rev. A* **38** 3721
- [17] Ramaswamy S, Nityananda R, Raghunathan V A and Prost J 1996 *Mol. Cryst. Liq. Cryst.* **288** 175
- [18] Hunter R J 1981 *Zeta Potential in Colloid Science* (London: Academic)
- [19] Chandrasekhar S 1992 *Liquid Crystals* 2nd edn (Cambridge: Cambridge University Press)